J Nanostruct 15(4): 1558-1568, Autumn 2025

RESEARCH PAPER

Investigating the Impact of Mycosynthesised Iron Nanoparticles Against *Candida Albicans* Cells and Studying Their Antioxidants Activity

Amer H. Abbas [1,2*], ***Shatha Ali Shafiq*** [2], ***Azhar M. Haleem*** [3]

[1] *Department of Applied Science, University of Technology, Baghdad, Iraq*

[2] *College of Science, Mustansiriyah University, Baghdad, Iraq*

[3] *Environmental Research Center,/ University of Technology, Baghdad, Iraq*

ARTICLE INFO

Article History:
Received 12 May 2025
Accepted 05 August 2025
Published 01 October 2025

Keywords:
Cell wall
Endophytic fungus
FeNPs
Nanomaterials

ABSTRACT

Mycosynthesizing Iron nanoparticles (FeNPs) are the focus of this investigation using the endophytic fungus *fusarium graminearum* isolated from *Salvia Rosmarinus* and testing the nanoparticle's action against *candida albicans* cells and antioxidant activity. First, the fungus was isolated and purified on Potato Dextrose Agar (PDA) from *Salvia Rosmarinus* leaves and stems, after that, fungal biomass was produced using a laboratory-prepared media, and the biomass was introduced to iron salt; Ferrous sulphate ($FeSO_4.7H_2O$) solution to mycosynthesis FeNPs. FeNPs were characterised using many techniques. A colour shift from yellowish-orange colour to dark brown is the first indicator of the FeNPs mycosynthesis. FeNPs were detected in UV–vis absorption spectra with a 303 nm band. XRD analyses prove the crystallinity phase of FeNPs with four distinctive peaks; at 2θ values of 24.84°, 33.52°, 39.12°, and 42.31°. FeNPs FTIR spectra showed absorption peaks from 3400 to 406.98 cm^1. The FE-SEM scans showed 45.89–80.05 nm spherical particles. The particles revealed a diameter of 86.79 nm (the average) with a size range spanning from 22.23 to 107.7 nm, according to AFM pictures and charts. FE-SEM technique is used to detect the impact of FeNPs on *Candida albicans* cells with a clear impact on its cell wall. FeNPs showed scavenging activity increased with concentration.

How to cite this article
Abbas A., Shafiq S., Haleem A. Investigating the Impact of Mycosynthesised Iron Nanoparticles Against Candida Albicans Cells and Studying Their Antioxidants Activity. J Nanostruct, 2025; 15(4):1558-1568. DOI: 10.22052/JNS.2025.04.006

INTRODUCTION

Nowadays, nano and microstructures (that is less than 100 nm), have acquired applications in several fields of science and technology, including physics, chemistry, biology, and biotechnology [1]. Nanoparticles are characterized by distinct chemical compositions, physical attributes, high ratios of surface area to volume, low melting points, strong photoconductivity, catalytic capabilities, and biological features [2]. To date, Iron nanoparticles (FeNPs) are innovative materials with distinctive physicochemical features, including high catalytic activity, strong magnetic, low toxicity, and the ability to absorb microwaves

* *Corresponding Author Email: amerabbas8080@gmail.com*

[3]. These particles have diverse applications, such as drug delivery, magnetic targeting, thermal ablation, hyperthermia, stem cell sorting and manipulation, gene therapy, food preservation, environmental remediation, antimicrobial agents, bioseparation, and treatment for cancer [4]. In biochemical applications, it is crucial to synthesize eco-friendly and non-toxic nanoparticles. Iron nanoparticles have been especially desired due to their low toxicity, as iron naturally exists in the body and can be tolerated in higher doses compared to other metals. Chemical and physical techniques in synthesizing nanoparticles have been deemed unsuitable for biochemical applications due to the production of hazardous compounds [5]. The biogenic path to NP synthesis provides a novel avenue to explore and identify new biological sources that can reduce metals to the nanoscale. Certain microorganisms, including bacteria, fungi, and plants, have been discovered to possess the ability to generate NPs. There is a limited number of publications on synthesizing NPs by endophytic microorganisms. This method is considered to be safe, nonhazardous, and ecologically friendly [6,7].

Among the biological agents, fungi have consistently played a prominent role in providing a more sustainable alternative to chemically synthesized nanoparticles, referred to as mycosynthesis [8]. The preference for the fungal synthesis of iron magnetic nanoparticles over other microorganisms is due to its easy handling, low cost, high tolerance towards heavy metals, and simplified downstream processing. Fungi have been reported to display increased variability in size, improved structural integrity, and a wider variety of dimensions in producing various nanoparticles [9,10]. Various fungi have been successfully employed for the biological production of nanoparticles. However, according to the available literature, it is evident that several species of *Fusarium* fungi are the prime to scientists [11].

Apart from that, reactive species are involved a participate in a plethora of other biological activities within every organism, notably cell maturation, immunological defence, and cytotoxicity against pathogens. Nevertheless, they have the potential to cause damage to proteins, lipids, DNA [12], and cell walls [13].

This study aimed to use the endophytic fungus *Fusarium graminearum* to synthesize FeNPs. FeNPs action against *candida albicans* cells and their antioxidant activity were analyzed.

MATERIALS AND METHODS

This study's chemicals and reagents were procured from the American company Sigma, Ltd. All the experiments were performed at the cell biology laboratory of the Applied Science Department at the University of Technology in Iraq.

Isolation and identification of Fusarium graminearum

Immediately after rinsing with running water, the *Salvia rosmarinus* leaves were submerged in double-distilled water for 10 minutes. To sterilise the leaves, we submerged them in 70% ethanol for three minutes, then 0.5% sodium hypochlorite (NaOCl) for one minute, and then another thirty seconds. Immersion in 70% ethanol. Finally, they rinsed three times with sterilized distilled water. Petri dishes with Potato Dextrose Agar (PDA) treated with chloramphenicol at a concentration of 250 mgL^{-1} were used for the cultivation of sterile leaf fragments measuring 0.5 cm. The plates were thereafter wrapped with parafilm and incubated at a temperature of 250 °C until the endophytic fungus became visible. In order, the developing hyphal tips from the plant segments were isolated and subjected to subculture to get a pure culture [15,16]. The identification of fungal endophytes was achieved using traditional identification protocols. Using macroscopic characteristics such as colony growth, form, and color, alongside microscopic characteristics like colony surface, texture, conidia, conidiophores, and hypha pigmentation [17]. The potential of *Fusarium graminearum* has been evaluated for its use in the synthesis of FeNPs.

Preparation of fungal extract

The inoculum was generated using a modified Wunder media [18]. The components of the medium included glucose (10 gL^{-1}), polypeptone (1 gL^{-1}), K_2HPO_4 (0.125 gL^{-1}), $(NH_4)_2SO_4$ (1 gL^{-1}), $MgSO_4 \cdot 7H_2O$ (0.5 gL^{-1}), KH2PO4 (0.875 gL^{-1}), $CaCl_2 \cdot 2H_2O$ (0.1 gL^{-1}), NaCl (0.1 gL^{-1}), $MnSO_4 \cdot H_2O$ (0.02 gL^{-1}), and $FeSO_4 \cdot 7H_2O$ (0.001 gL^{-1}). Each Erlenmeyer flask was enriched with 170 ml of medium, and six mm diameter discs of the fungus were added, which were previously cultured on PDA medium. The inoculated flasks underwent continuous agitation at a speed of 125 rpm at 28

°C for 7 days. After incubation, the fungal biomass was filtered and used in future experiments.

Iron Mycosynthesis

The harvested mycelia were separated from the culture broth by subjecting them to be centrifugated at 4500 rpm for 16 minutes. This operation was repeated three to four times, distilled water was used for each wash. Following a three-day incubation period at a temperature of 28.2 °C,100 ml of fungal mycelia is mixed with 100 ml of deionized water containing 0.4mg of Ferrous sulphate ($FeSO_4.7H_2O$) [19].

Iron Nanoparticles Characterization

Prior to characterization, ethanol was used for FeNPs extraction from fungal mycelia. Subsequently, ultrasonic dispersion was employed. The study focuses on the bioreduction process of Iron ions in mycelium solution, which is transformed into Iron nanoparticles. The solution changed color within a particular period, suggesting the conversion of Iron ions into FeNPs. A UV-visible spectrophotometer (LAMBDA 365 spectrophotometer-PerkinElmer, Waltham, MA, USA) was used to conduct absorption measurements in the 200 to 800 nm wavelength range. X-ray diffractograms (XRD) were applied using an X-ray diffractometer (HAOYUAN, Zhejiang, China) at 40 kilovolts and 40 milliamperes with Cu(Kilo α) radiation (wavelenght = 1.5406 Å). Diffraction angle (2θ) scanned from 10° to 80° to estimate the diameter and size of the nanoparticles by measuring their peak width and length. The surface charge and persistence were conducted using a Zeta potential analyzer (Zeta, Brookhaven, Deklab County, GA, USA). Fourier Transform Infrared Spectroscopy analysis used an FTIR spectrometer (PerkinElmer, Waltham, MA, USA) to determine the functional groups generated in the FeNPs. The study was conducted at ambient temperature and recorded within the spectral region of 400-4000 cm^{-1}. FeNPs were mixed with potassium bromide at a ratio of 1:100. Then, the functional groups were based on vibrational mode. The shape of the biosynthesized FeNPs was examined using a Field Emission Scanning Electron Microscope (Inspect F50-FE-SEM, FEI, Eindhoven, The Netherlands) with energy-dispersive X-ray (EDX) attachment to analyze the composition and confirm the presence of elemental iron in its natural form. Furthermore, the surface morphology, aggregation, shape, size, and distance of biosynthesized FeNPs were examined using Atomic Force Microscopy (NaioAFM, Nanosurf AG, Liestal, Switzerland) with AFM image analysis software [20, 21].

Treating Candida albicans *cells with FeNPs and detecting their effects on the surface morphology*

After treating Candida albicans cells with FeNPs, the changes in surface and cellular appearance

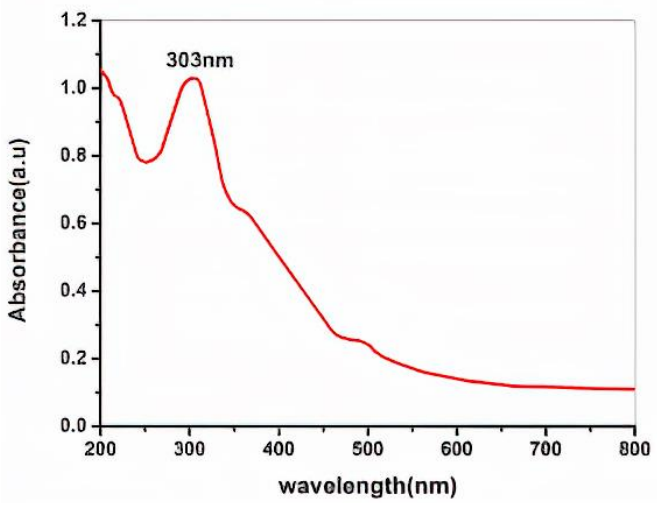

Fig. 1. UV–Vis spectroscopy of mycosynthesized FeNPs.

were examined using FE-SEM. Harvested cells were rinsed by PBS buffer to eradicate the medium, and then fixed with 2% glutaraldehyde in 0.1 M phosphate buffer for 3 hours at 25°C. The cells were cultured either without or with the nanoparticles at a concentration of 40 µg/mL until they reached the mid-exponential phase. The cells were washed with phosphate buffer (pH 7.2) two to three times before being postfixed with 1% OsO_4 in 0.1 M phosphate buffer for 1 hour at 4°C to prepare them for FSEM, a portion of the cells that had been treated as described above was dehydrated in acetone, then placed onto a round glass coverslip that had been coated with hexamethyldisilazane, allowed to dry, and finally sputtered with gold, The cells were then observed under FE-SEM with a resolution of 3.0 nm at 30 kV and a magnification of 7–1,000,07 [13,22].

Antioxidant activity

The scavenging activities of FeNPs were assessed using stable DPPH radicals [23]. Adding 0.5 ml of FeNPs at various concentrations (0.0, 0.01, 0.1, 1, 10, and 100 μgml^{-1}) onto DPPH solution (0.5 millilitres of diphenylpicrylhydrazyl and 3.3 millilitres of 100% ethanol were combined to create the DPPH solution.). Spectroscopy was employed to determine the alteration in color at a specific wavelength of 515 nm, while the sample was subjected to a temperature of 25°C for 90 min. The blank solution was made by combining 0.5 ml of the sample with 3.3 ml of 100% ethanol. A control was employed, consisting of a tube containing a mixture of 100% ethanol (3.3 ml) and DPPH (0.5 ml). The percentage of elimination was determined using an equation for antioxidant activity.

$$\text{scavengingactivities} = 100 - \frac{1-\text{sample absorbency}}{\text{control absorbency}} \times 100\%$$

RESULTS AND DISCUSSION

Endophytic fungi derived from medicinal plants, mostly belonging to the Ascomycota and their sexual forms, have been collected. These fungi, commonly called herbaceous plants, can infect and establish a symbiotic relationship with many herbaceous plants worldwide [24, 25].

Applying endophytes in a biosynthetic approach is an innovative method for developing safe and economical technologies for NP production [26]. Fungi have the ability to generate enzymes and metabolites that function as reductive and capping agents. enabling them to create metal NPs with stable and controlled shapes. Research has demonstrated that enzymes or metabolites produced by fungi can reduce the metallic content of NPs by interfering with the main reaction that is dependent on the reduction or oxidation of the substrate. So, this makes it easier to make colloidal structures. [27].

The bottom-up approach uses fungi to reduce FeNPs, which are advantageous over other organisms. Their proteins and enzymes, such as reductive, can be used for fast and sustainable nanoparticle synthesis. Nevertheless, the top-

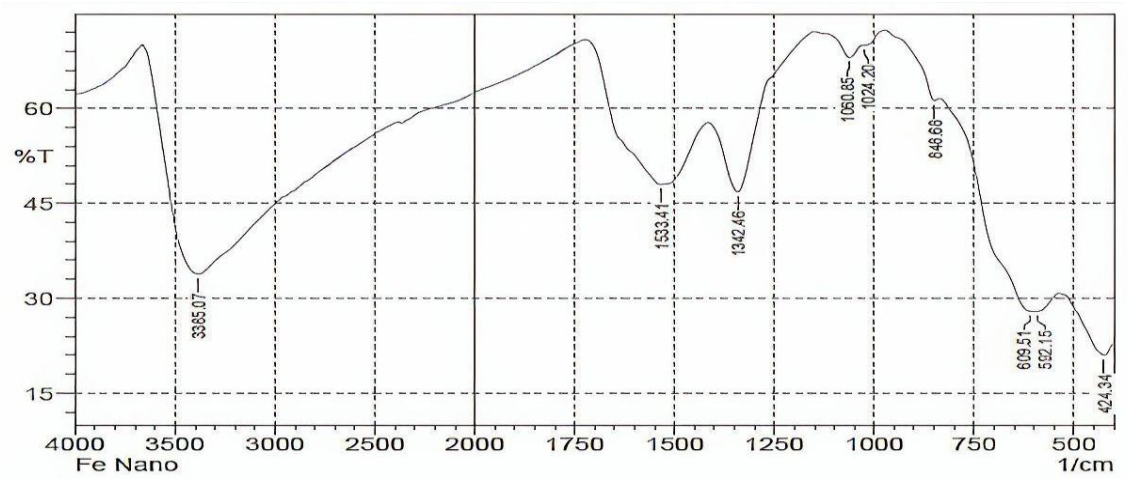

Fig. 2. FTIR spectrum of mycosynthesised FeNPs.

down approaches aren't as suitable as the bottom-up approaches for generating particles of petite sizes. In bottom-up methods, nanostructures are constructed by adding atoms, molecules, or clusters. This enables us to produce and design materials with predefined features [28]. The biosynthesis of FeNPs can be categorized into two methods: (i) intracellular and (ii) extracellular mechanisms. However, extracellular synthesis offers more advantages owing to its simplified downstream processing [29]. During extracellular synthesis, Iron ions underwent reduction to form FeNPs. This process occurs in the presence of extracellular enzymes, secondary metabolites, and biomolecules created by fungal cells [30]. However, the biosynthesis of NPs by fungi requires three steps: gathering metal ions near fungal cells, releasing enzymes that reduce iron ions, and stabilizing NPs using fungal peptides and proteins [31].

Mycosynthesised nanoparticle characterization and analysis

UV-Vis Spectrophotometry

The first sign of FeNPs synthesis was the color shift and UV-Vis spectroscopic detection of maximal SPR. The transition of color from yellowish-orange to dark brown during the production of FeNPs might be ascribed to surface Plasmon resonance (SPR), which is a distinctive characteristic of NPs. The prepared FeNPs were characterized by measuring their absorbance using UV-Vis spectrometry in the 200 to 800nm wavelength range, as shown in Fig. 1. The peak observed at 303nm indicated the formation of FeNPs by the endophytic fungi. Furthermore, the broadening of the peak is related to several distinct factors; the shape, size, and polydispersity of NPs [32], These findings are in line with the previously documented absorption peak of FeNPs at 300 nm synthesized from *Penicillium oxalicum* [33]. The endophytic fungal isolate of *Fusarium graminearum* had the maximum color intensity with an absorption peak of 303 nm, which aligns with the surface Plasmon resonance (SPR) for FeNPs.

FT-IR Analysis

The FTIR spectra of iron NPs produced using *Fusarium graminearum* are shown in Fig. 2. In order to determine whether iron NPs contained phytocompounds derived from a fungal extract and whether they had a role in the reduction of iron ions, Fourier transform infrared (FTIR) tests were conducted. The transmittance peaks detected at 424.34 cm^{-1}, 609.51 cm^{-1}, 848.68 cm^{-1},1024.20 cm^{-1},1060.85 cm^{-1}, 1342.46 cm^{-1}, 1533.41 cm^{-1}, 3385.07 cm^{-1}, respectively. The vibrational frequency at 609.51 cm^{-1} is linked with O_2 (Fe–O) stretching bonds [34]. A weak peak obtained at 1060.85 cm^{-1} corresponds to the stretching vibrations of C-O-C as reported in reference [35].

The bands observed at 3385.07 cm^{-1} and 1533.41 cm^{-1} correspond to O–H and C=C stretching vibrations in water, respectively.

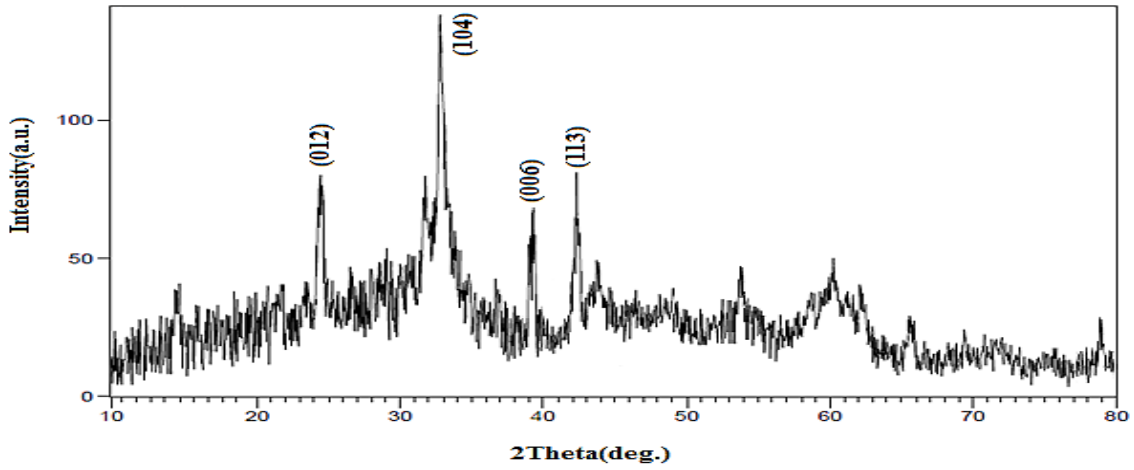

Fig. 3. X-ray diffraction pattern of mycosynthesised FeNPs.

The band at 1342.46 cm^{-1} is equivalent to the stretching vibration of C–N bonds in aliphatic and aromatic amines, this band indicates the existence of phenolic compounds that might be involved in the NP formation. Thus, fungal extracts include diverse organic compounds and act as a great supply of capping and reducing agents in producing FeNPs [36]. The –OH groups are implicated in the reduction process by oxidizing them to carbonyl groups. Additionally, particle stability is achieved by the involvement of carbonyl and carboxylate groups [37].

XRD Analysis

The XRD is the most efficient technique for analyzing materials. Findings and patterns in the XRD analysis's output tell us anything about the particles' nature. The X-ray diffraction (XRD) pattern of the FeNPs obtained by mycosynthesis is presented in Fig. 3. The pattern exhibited absorption peaks corresponding to the crystallographic planes (012), (104), (006), and (113). These peaks aligned with the Bragg diffraction at 2θ values of 24.84°, 33.52°, 39.12°, and 42.31° indicating the presence of the crystalline phase of FeNPs. This observation was compared to the JCPDS standard card No. 06-0362. These findings are consistent with those observed in previous studies on FeNPs [38].

FE-SEM micrographs of Iron nanoparticles

Fig. 4 exhibits representative images at various degrees of magnification. Image A provides a

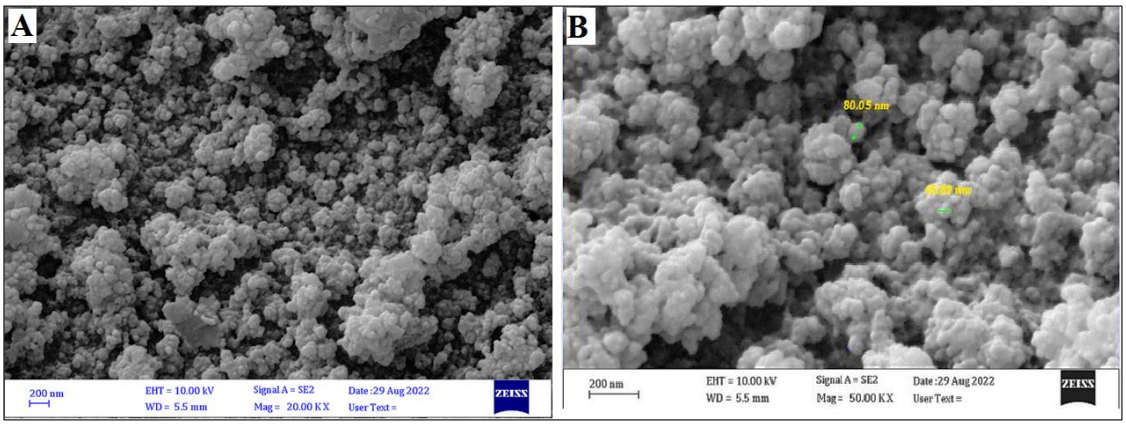

Fig. 4. SEM images and particle size measurements of mycosynthesised FeNPs.

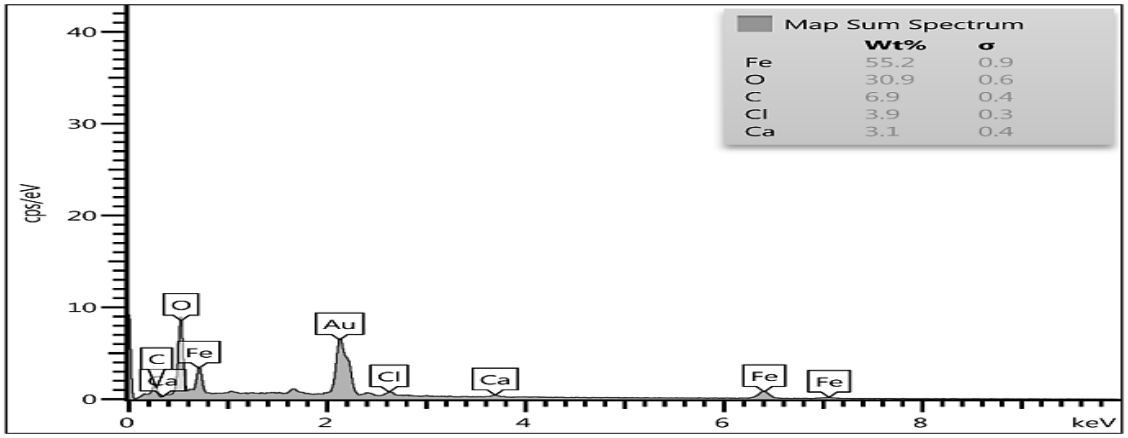

Fig. 5. EDX spectra for FeNPs.

general overview (20.00k) of mycosynthesized FeNPs, while image-B offers a higher magnification (50.00k). The SEM technique was used to investigate the size, shape, and aggregation of FeNPs, which influence their metabolic processes. It is evident that most of the FeNPs are spherical with a smooth surface and show some particle aggregation. The dimensions of the structures ranged from 45.89 nm to 89.05 nm, which is related to the findings of the XRD analysis. The activity of the NPs

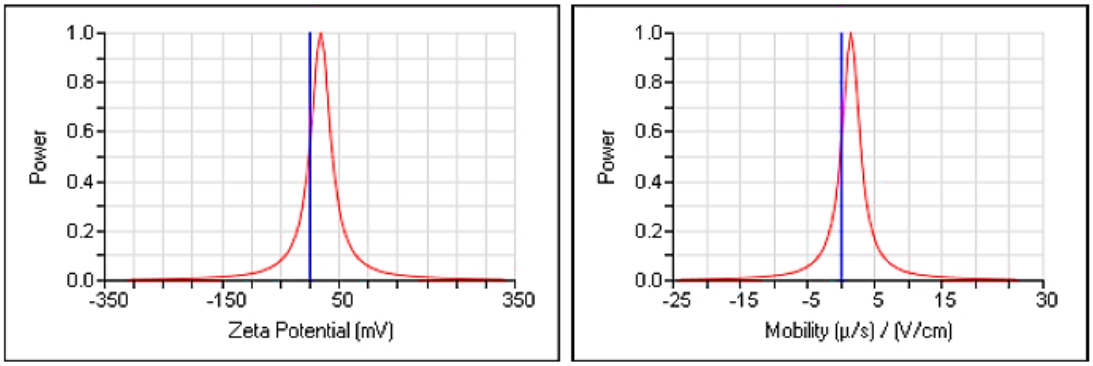

Fig. 6. Zeta potentials and dynamic light scattering analyses of FeNPs

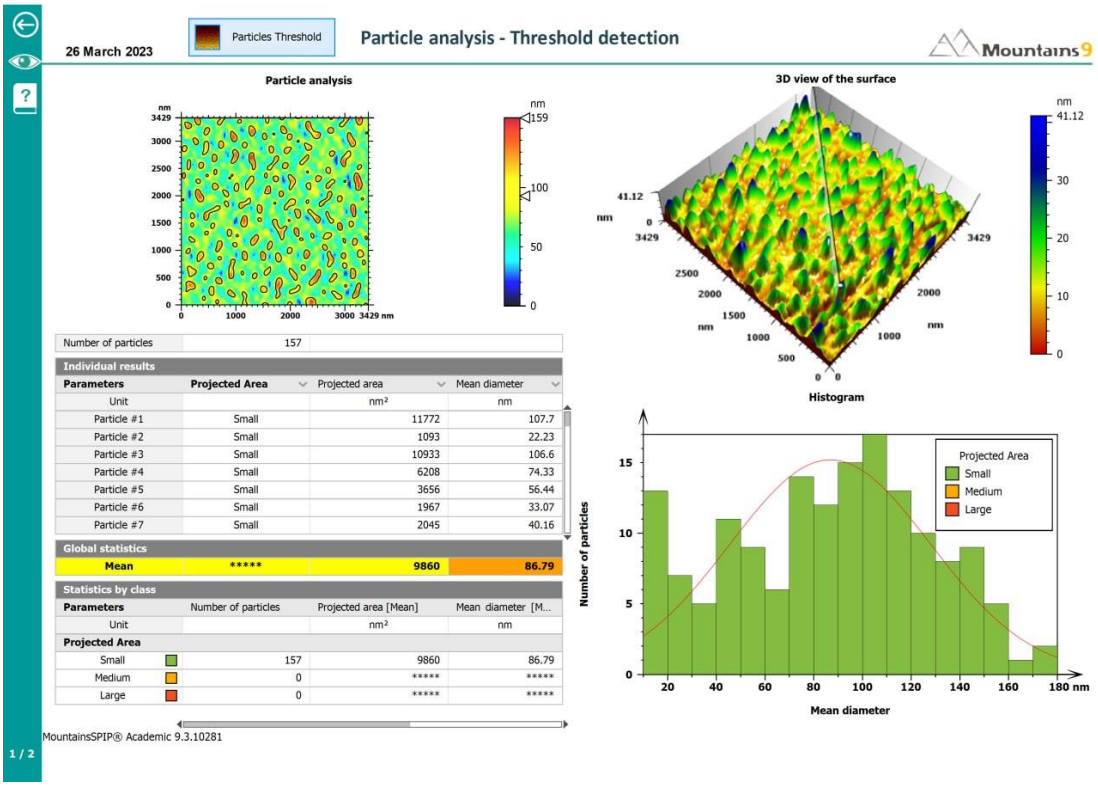

Number of particles	157		
Individual results			
Parameters	**Projected Area**	Projected area	Mean diameter
Unit		nm²	nm
Particle #1	Small	11772	107.7
Particle #2	Small	1093	22.23
Particle #3	Small	10933	106.6
Particle #4	Small	6208	74.33
Particle #5	Small	3656	56.44
Particle #6	Small	1967	33.07
Particle #7	Small	2045	40.16
Global statistics			
Mean	*****	9860	86.79
Statistics by class			
Parameters	Number of particles	Projected area [Mean]	Mean diameter [M...
Unit		nm²	nm
Projected Area			
Small	157	9860	86.79
Medium	0	*****	*****
Large	0	*****	*****

Fig. 7. AFM topography images of biosynthetic FeNP .

increased as the size diminished. Additionally, the shape of NPs impacts their behavior [39,40]. The observed aggregation of FeNPs may be attributed to the electrostatic contact between layers of the NP surface. Furthermore, NPs tend to form agglomerates suspended due to their elevated surface area-to-volume ratio [41].

The energy-dispersive X-ray (EDX) confirms the existence of iron elements in the compound. The EDX spectra demonstrated the presence of iron peaks in three separate regions (0.7, 6.4, and 7.0). The weight percentage of Fe in the FeNPs was 55.2% of the total sample components, with 30.9% of oxygen, 6.9% of carbon, with a minimal percentage of calcium and chlorine were also found in these FeNPs sample, which may be attributed to the fungal extract (Fig. 5) [42].

Size and Zeta Potential Measurements and Atomic Force Microscope (AFM)

The findings of the values of the polydispersity index (PDI) and hydrodynamic diameter (DLS) for FeNPs were shown in Fig. 6. It shows the mean size was 63.7 nm with PDI of 0.35, confirming the nanoscale size of the FeNPs. The PDI is an essential indicator for evaluating the distribution of particle sizes in FeNPs [46].

Shafiq et al. (2016) [7] and Aja et al. (2018) [47] described *Fusarium graminaerum* biosynthesised FeNPs in various sizes, which were sluggish to consume AFM.

Cellular and intracellular imaging

To investigate how 40 µg/mL (MIC90) FeNPs affected the surface morphology of *Candida albicans* cells, Fe-SEM was employed. Untreated cells seemed to have a smooth exterior in the matching SEM micrographs (Fig. 8), while cells treated with FeNPs displayed noticeable surface changes and outer cell walls that were rough and wrinkled (Fig. 9).

Disruptions to membrane potential, cellular ultrastructure, and apoptosis triggering were the only negative effects of Nps on Candida cells

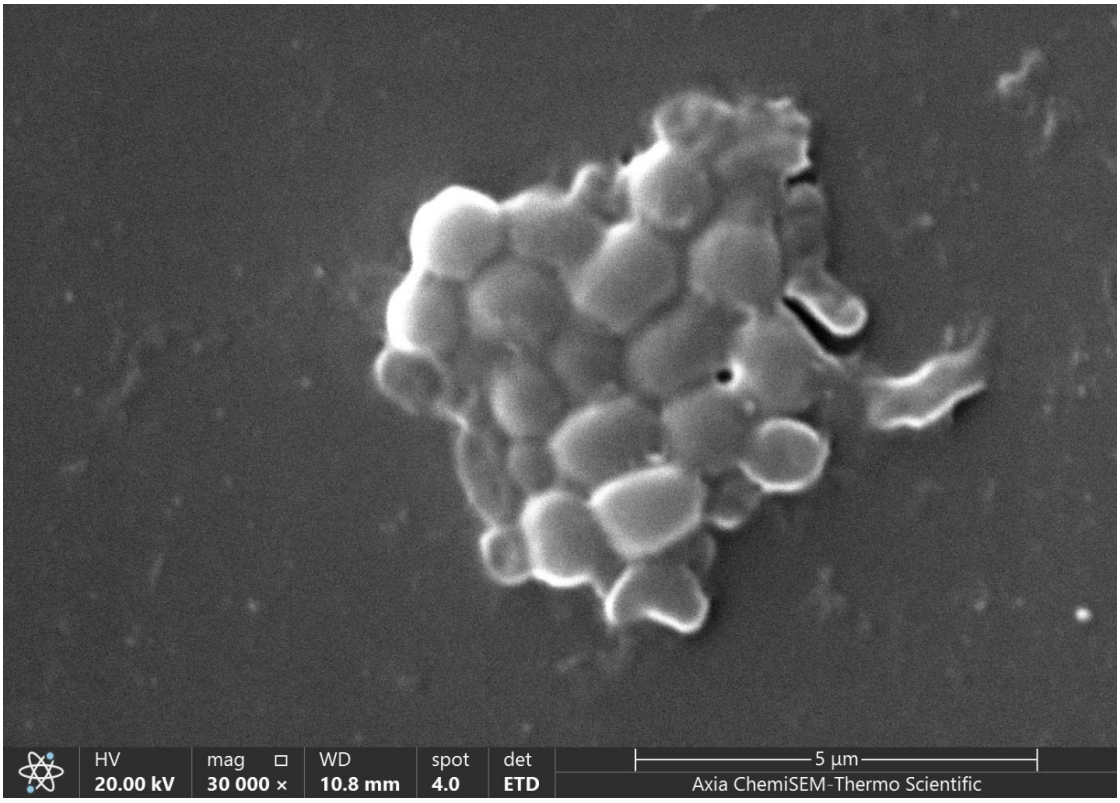

Fig. 8. FE- SEM micrographs untreated (no FeNps) *Candida albicans* cells showing the smooth surface of the cell wall.

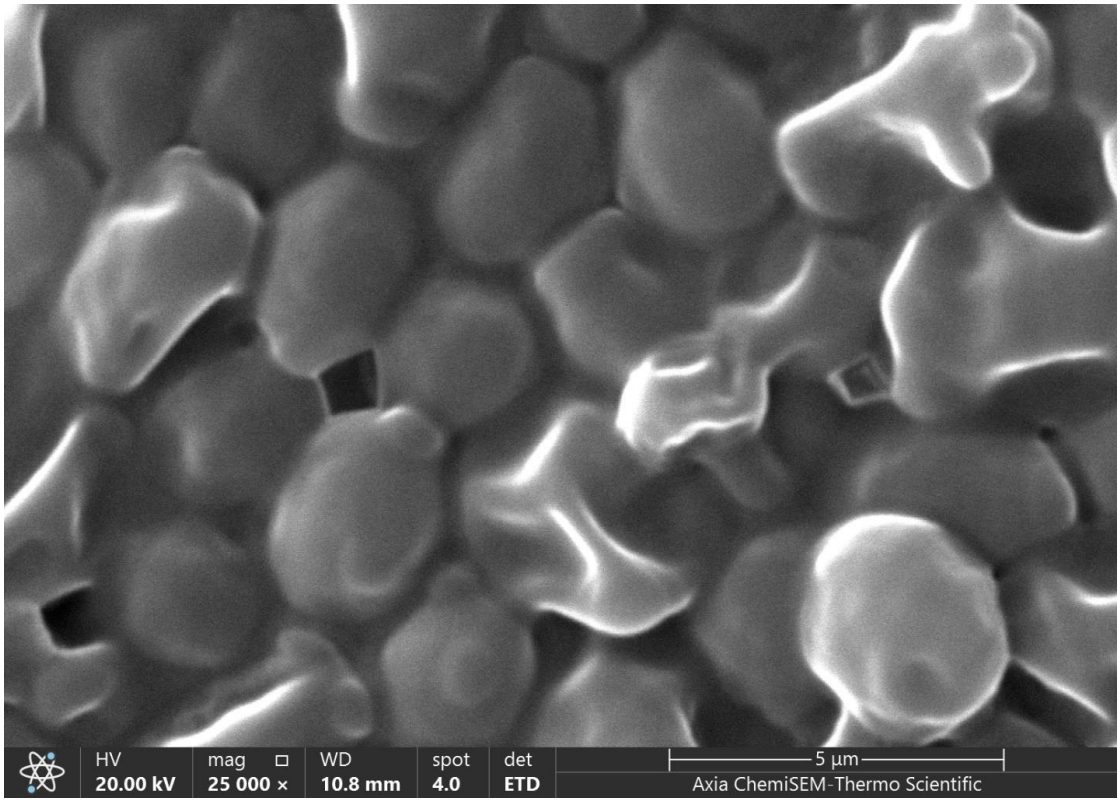

Fig. 9. SEM micrographs for *Candida albicans* cells treated with FeNps.

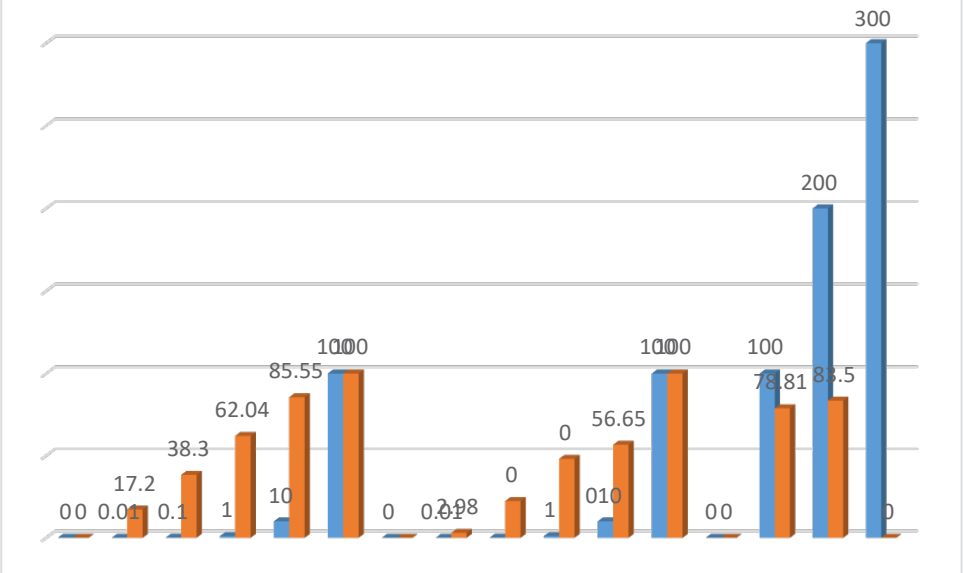

Fig. 10. Antioxidant effect of FeNPs and Ascorbic acid.

that were documented in a small number of investigations [44].

The cell wall and membrane of *Candida albicans* cells were clearly visible and undamaged when no FeNp treatment was applied (control) (Fig. 8). In contrast, our FE-SEM findings were supported by Fig. 9, which showed that *Candida* cells treated with 40 µg/mL FeNps had reduced cell wall and membrane integrity, which is consistent with prior results [45]. Pathogenic fungi rely on their cell envelope, which consists of the cell wall and membrane, to be stable, rigid, and resistant to physical stressors [46]. The physical condition and, by extension, the fluidity of the cell membrane may be affected by the effects of FeNps on the cell wall and membrane.

Antioxidant action of FeNps

The stable free radical DPPH, at room temperature, exhibits a rich violet colour with a 517 nm, which represents the absorbed wavelength when dissolved in organic solvents. The inclusion of selenium nanoparticles (SeNPs) in the analysis resulted in a decrease in DPPH stability and a change in colour from violet to yellow, which can be attributed to the phenolic OH groups present [47].

The scavenging of DPPH was seen to be directly related to the concentrations of the FeNPs. Specifically, at concentrations of 0.01, 0.1, 1, 10, and 100 gm/ml of FeNPs, the DPPH free radicals' scavenging capabilities were found to be 4.48%, 11.315 24.6%, 46.9%, and 100%, respectively (Fig. 10). FeNPs2 demonstrated the most pronounced scavenging activity when present at a concentration of 100%.

CONCLUSION

It may be inferred that the use of endophytic fungi fusarium for the biosynthesis of FeNPs is a straightforward, expeditious, and efficient method with a diameter of 45.89–80.05 nm nanometers; furthermore, the utilisation of fungal cell filtrate renders it even more environmentally sustainable and less detrimental to human health and the surrounding ecosystem. It has been proven that iron nanoparticles (FeNPs) exhibit scavenging activity increased with concentration.

CONFLICT OF INTEREST

The authors declare that there is no conflict of interest regarding the publication of this manuscript.

REFERENCES

1. Reguyal F, Sarmah AK, Gao W. Synthesis of magnetic biochar from pine sawdust via oxidative hydrolysis of FeCl2 for the removal sulfamethoxazole from aqueous solution. J Hazard Mater. 2017;321:868-878.
2. Digest Journal of Nanomaterials and Biostructures.
3. Guo J, Wang R, Tjiu WW, Pan J, Liu T. Synthesis of Fe nanoparticles@graphene composites for environmental applications. J Hazard Mater. 2012;225-226:63-73.
4. Ebrahiminezhad A, Zare-Hoseinabadi A, Sarmah AK, Taghizadeh S, Ghasemi Y, Berenjian A. Plant-Mediated Synthesis and Applications of Iron Nanoparticles. Mol Biotechnol. 2017;60(2):154-168.
5. Kianpour S, Ebrahiminezhad A, Mohkam M, Tamaddon AM, Dehshahri A, Heidari R, et al. Physicochemical and biological characteristics of the nanostructured polysaccharide-iron hydrogel produced by microorganism Klebsiella oxytoca. J Basic Microbiol. 2016;57(2):132-140.
6. Mahdavi M, Namvar F, Ahmad M, Mohamad R. Green Biosynthesis and Characterization of Magnetic Iron Oxide (Fe_3O_4) Nanoparticles Using Seaweed (Sargassum muticum) Aqueous Extract. Molecules. 2013;18(5):5954-5964.
7. Abdeen M, Sabry S, Ghozlan H, El-Gendy AA, Carpenter EE. Microbial-Physical Synthesis of Fe and Fe_3O_4 Magnetic Nanoparticles Using Aspergillus niger YESM1 and Supercritical Condition of Ethanol. Journal of Nanomaterials. 2016;2016:1-7.
8. Biosynthesis of Silver Nanoparticles Using Saccharomyces Cerevisiae with Different pH and Study of Antimicrobial Activity against Bacterial Pathogens. Chemical Science Transactions. 2016.
9. Khandel P, Shahi SK. Mycogenic nanoparticles and their bio-prospective applications: current status and future challenges. Journal of Nanostructure in Chemistry. 2018;8(4):369-391.
10. Messaoudi O, Bendahou M. Biological Synthesis of Nanoparticles Using Endophytic Microorganisms: Current Development. Nanotechnology and the Environment: IntechOpen; 2020.
11. Rai M, Bonde S, Golinska P, Trzcińska-Wencel J, Gade A, Abd-Elsalam KA, et al. Fusarium as a Novel Fungus for the Synthesis of Nanoparticles: Mechanism and Applications. Journal of Fungi. 2021;7(2):139.
12. Schieber M, Chandel Navdeep S. ROS Function in Redox Signaling and Oxidative Stress. Curr Biol. 2014;24(10):R453-R462.
13. Musimun C, Papiernik D, Permpoonpattana P, Chumkaew P, Srisawat T. Synergy of green-synthesized silver nanoparticles and Vatica diospyroides fruit extract in inhibiting Gram-positive bacteria by inducing membrane and intracellular disruption. J Exp Nanosci. 2022;17(1):420-438.
14. Parcheta M, Świsłocka R, Orzechowska S, Akimowicz M, Choińska R, Lewandowski W. Recent Developments in Effective Antioxidants: The Structure and Antioxidant Properties. Materials. 2021;14(8):1984.
15. Ganesan V, Hariram M, Vivekanandhan S, Muthuramkumar S. Periconium sp. (endophytic fungi) extract mediated sol-gel synthesis of ZnO nanoparticles for antimicrobial and antioxidant applications. Mater Sci Semicond Process. 2020;105:104739.
16. Iamanaka BT, Taniwaki MH, Vicente E, Menezes HC. Fungi producing ochratoxin in dried fruits. Advances in

Experimental Medicine and Biology: Springer US; 2006. p. 181-188.
17. Selim KA. Biology of Endophytic Fungi. Current Research in Environmental and Applied Mycology. 2012;2(1):31-82.
18. Morales-Mendoza AG, Flores-Trujillo AKI, Ramírez-Castillo JA, Gallardo-Hernández S, Rodríguez-Vázquez R. Effect of Micro-Nanobubbles on Arsenic Removal by Trichoderma atroviride for Bioscorodite Generation. Journal of Fungi. 2023;9(8):857.
19. Ranjani S, Kathun UR, Hemalatha S. Silver Decorated Myconanoparticles Control Growth and Biofilm Formation in Uropathogenic E. coli. Applied Biochemistry and Biotechnology. 2021;194(1):504-516.
20. Ajah HA, Khalaf KJ, Hasan AM. Extracellular Biosynthesis of Silver Nanoparticles Using Sphingomonas paucimobilis, Serratia Sp. And Pseudomonas aeruginosa and Their Antimicrobial Activity. Indian Journal of Public Health Research & Development. 2018;9(12):911.
21. Ibraheem DR, Hussein NN, Sulaiman GM, Mohammed HA, Khan RA, Al Rugaie O. Ciprofloxacin-Loaded Silver Nanoparticles as Potent Nano-Antibiotics against Resistant Pathogenic Bacteria. Nanomaterials. 2022;12(16):2808.
22. Srisawat T, Sukpondma Y, Graidist P, Chimplee S, Kanokwiroon K. The dose dependent in vitro responses of MCF-7 and MDA-MB-231 cell lines to extracts of Vatica diospyroides symington type SS fruit include effects on mode of cell death. Pharmacogn Mag. 2015;11(42):148.
23. Khane Y, Benouis K, Albukhaty S, Sulaiman GM, Abomughaid MM, Al Ali A, et al. Green Synthesis of Silver Nanoparticles Using Aqueous Citrus limon Zest Extract: Characterization and Evaluation of Their Antioxidant and Antimicrobial Properties. Nanomaterials. 2022;12(12):2013.
24. Fitriarni D, Kasiamdari RS. Isolation and Identification of Endophytic Fungi from Leave and Stem of Calopogonium mucunoides. Journal of Tropical Biodiversity and Biotechnology. 2018;3(1):30.
25. Dinodia N, Sharma RK, Gond VK, Dinodia N. Endophytic Fungi Isolation and Identification from Stem of Tinospora Cordifolia. Research Square Platform LLC; 2022.
26. Gange AC, Eschen R, Wearn JA, Thawer A, Sutton BC. Differential effects of foliar endophytic fungi on insect herbivores attacking a herbaceous plant. Oecologia. 2011;168(4):1023-1031.
27. Bhattacharjee S, Debnath G, Das AR, Saha AK, Das P. Characterization of silver nanoparticles synthesized using an endophytic fungus, Penicillium oxalicum having potential antimicrobial activity. Advances in Natural Sciences: Nanoscience and Nanotechnology. 2017;8(4):045008.
28. Adebayo EA, Azeez MA, Alao MB, Oke AM, Aina DA. Fungi as veritable tool in current advances in nanobiotechnology. Heliyon. 2021;7(11):e08480.
29. Mohamed HI, Fawzi EM, Abd-Elsalam KA, Ashry NA, Basit A. Endophytic fungi-derived biogenic nanoparticles: Mechanisms and applications. Fungal Cell Factories for Sustainable Nanomaterials Productions and Agricultural Applications: Elsevier; 2023. p. 361-391. http://dx.doi.org/10.1016/b978-0-323-99922-9.00024-6
30. Rizwan M, Ali S, Ali B, Adrees M, Arshad M, Hussain A, et al. Zinc and iron oxide nanoparticles improved the plant growth and reduced the oxidative stress and cadmium concentration in wheat. Chemosphere. 2019;214:269-277.
31. Gezaf S, Hamedo H, Ibrahim A, Mossa M. Mycosynthesis of silver nanoparticles by endophytic Fungi: Mechanism, characterization techniques and their applications. Microbial Biosystems. 2022;7(2):48-65.
32. Zhao X, Zhou L, Riaz Rajoka MS, Yan L, Jiang C, Shao D, et al. Fungal silver nanoparticles: synthesis, application and challenges. Crit Rev Biotechnol. 2017;38(6):817-835.
33. Rajendran K, Karunagaran V, Mahanty B, Sen S. Biosynthesis of hematite nanoparticles and its cytotoxic effect on HepG2 cancer cells. Int J Biol Macromol. 2015;74:376-381.
34. Mathur P, Saini S, Paul E, Sharma C, Mehtani P. Endophytic fungi mediated synthesis of iron nanoparticles: Characterization and application in methylene blue decolorization. Current Research in Green and Sustainable Chemistry. 2021;4:100053.
35. Devatha CP, Thalla AK, Katte SY. Green synthesis of iron nanoparticles using different leaf extracts for treatment of domestic waste water. Journal of Cleaner Production. 2016;139:1425-1435.
36. Rajiv P, Bavadharani B, Kumar MN, Vanathi P. Synthesis and characterization of biogenic iron oxide nanoparticles using green chemistry approach and evaluating their biological activities. Biocatalysis and Agricultural Biotechnology. 2017;12:45-49.
37. Saranya S, Vijayarani K, Pavithra S. Green Synthesis of Iron Nanoparticles using Aqueous Extract of Musa ornata Flower Sheath against Pathogenic Bacteria. Indian J Pharm Sci. 2017;79(5).
38. Madivoli ES, Kareru PG, Maina EG, Nyabola AO, Wanakai SI, Nyang'au JO. Biosynthesis of iron nanoparticles using Ageratum conyzoides extracts, their antimicrobial and photocatalytic activity. SN Applied Sciences. 2019;1(5).
39. Da'na E, Taha A, Afkar E. Green Synthesis of Iron Nanoparticles by Acacia nilotica Pods Extract and Its Catalytic, Adsorption, and Antibacterial Activities. Applied Sciences. 2018;8(10):1922.
40. Salem SS, Fouda A. Green Synthesis of Metallic Nanoparticles and Their Prospective Biotechnological Applications: an Overview. Biol Trace Elem Res. 2020;199(1):344-370.
41. Chandramohan S, Sundar K, Muthukumaran A. Reducing agents influence the shapes of selenium nanoparticles (SeNPs) and subsequently their antibacterial and antioxidant activity. Materials Research Express. 2019;6(8):0850i0852.
42. Bae E, Lee B-C, Kim Y, Choi K, Yi J. Effect of agglomeration of silver nanoparticle on nanotoxicity depression. Korean J Chem Eng. 2012;30(2):364-368.
43. Bhuiyan MSH, Miah MY, Paul SC, Aka TD, Saha O, Rahaman MM, et al. Green synthesis of iron oxide nanoparticle using Carica papaya leaf extract: application for photocatalytic degradation of remazol yellow RR dye and antibacterial activity. Heliyon. 2020;6(8):e04603.
44. Selvaraj M, Pandurangan P, Ramasami N, Rajendran SB, Sangilimuthu SN, Perumal P. Highly Potential Antifungal Activity of Quantum-Sized Silver Nanoparticles Against Candida albicans. Applied Biochemistry and Biotechnology. 2014;173(1):55-66.
45. Lara HH, Romero-Urbina DG, Pierce C, Lopez-Ribot JL, Arellano-Jiménez MJ, Jose-Yacaman M. Effect of silver nanoparticles on Candida albicans biofilms: an ultrastructural study. Journal of Nanobiotechnology. 2015;13(1).
46. Chaffin WL, López-Ribot JL, Casanova M, Gozalbo D, Martínez JP. Cell Wall and Secreted Proteins of Candida albicans: Identification, Function, and Expression. Microbiology and Molecular Biology Reviews. 1998;62(1):130-180.
47. Deligiannakis Y, Sotiriou GA, Pratsinis SE. Antioxidant and Antiradical SiO_2 Nanoparticles Covalently Functionalized with Gallic Acid. ACS Applied Materials & Interfaces. 2012;4(12):6609-6617.